Tripodal O-N-O *bis*-Phenolato Amine Titanium(IV) Complexes Show High *In Vitro* Anti-Cancer Activity

Mohammed Abid,[a,d] Ryan Nouch,[d] Tracey D. Bradshaw,[b] William Lewis,[c,d] and Simon Woodward*[d]

[a] M. Abid, Department of Chemistry, College of Science, University of Anbar, Western side of Ramadi City, Anbarshire (Republic of Iraq)
Emails: aboyazenabid@gmail.com and mohammed.abid@nottingham.ac.uk

[b] Associate Prof. Dr. T. D. Bradshaw, School of Pharmacy, Centre for Biomolecular Sciences, University Park, Nottingham, NG7 2RD (United Kingdom)
Email: tracey.bradshaw@nottingham.ac.uk

[c] Present address: Dr. W. Lewis, School of Chemistry, The University of Sydney, Eastern Avenue, Sydney, NSW 2006 (Australia)
Email: w.lewis@sydney.edu.au

[d] M. Abid, Dr. W. Lewis, R. Nouch, Prof. Dr. S. Woodward, GSK Carbon Neutral Laboratories for Sustainable Chemistry, University of Nottingham, Triumph Road, Nottingham, NG7 2TU (United Kingdom)
Email: simon.woodward@nottingham.ac.uk

Supporting information for this article is available (end of manuscript)

Abstract: The octahedral titanium(IV) complexes *trans*,*mer*-[Ti{R^3N(CH$_2$C$_6$H$_2$-2-O-4-R^2-6-R^1)$_2$}$_2$] (R^1 = Me, OMe, Cl; R^2 = Me, OMe, F, Cl; R^3 = Me, Et; not all combinations) are synthesised in two steps from simple phenols in 36-53% overall yield. The highly crystalline (4 X-ray structures) complexes are active against MCF-7 (breast) and HCT-116 (colon) cancer cell lines showing widely varying GI$_{50}$ values in the range 1-100 μM depending on R^1-R^3. Highest activities are realised when R^1 = OMe and R^2, R^3 = Me (GI$_{50}$ ~1 μM for MCF-7 and 2-3 μM for HCT-116). These are respectively 8× and 3× times greater than the activities of cisplatin in the same cell lines. These titanium complexes show some significant selectivity for cancer cell lines; up to 7× higher in MCF-7 compared to non-cancer (MRC-5) fibroblast cells. Details of cellular mode of action indicators (cell cycle perturbation, Annexin V, γ-H2AX, and caspase studies) that point to an apoptosis mode for the most active compound (R^1 = OMe and R^2, R^3 = Me) are also reported.

Mohammed Abid, Ryan Nouch, Tracey Bradshaw, William Lewis, Simon Woodward – Full paper for EJIC

Introduction

In 1969, cisplatin [*cis*-diamminedichloroplatinum(II)] first emerged as a cancer therapy, subsequently becoming one of the most popular antineoplastic (cytotoxic) agents employed against human ovarian, testicular, head, neck and bladder carcinomas. Although cisplatin possesses potential against most carcinomas, its toxic side-effects (myelotoxicity and nephrotoxicity) and problems with resistance soon became apparent.[1] Because of such issues, alternative metal complexes have also been explored for anti-cancer activity.[2] These related metal complexes can show mechanisms of action other than the DNA binding seen for cisplatin depending on their metal acidity/oxidation state and their supporting ligands.[3] In particular, titanium(IV) complexes have recently appeared showing activities higher or comparable to cisplatin and its Pt-based derivatives and these are thought to be promising anticancer drug candidates.[4] Unfortunately, progress towards potential clinical candidates has been hindered by a lack of understanding of the mechanism(s) of action of titanium agents.[5] Initial investigations in this area focused on titanocene dichloride Cp_2TiCl_2 (Cp = η-C_5H_5) and this candidate reached clinical trial (although its low efficacy did not allow it to progress beyond phase II). One of the problems in deriving the cellular mode of action of Cp_2TiCl_2, and related titanium(IV) complexes, is that while partial ligand hydrolysis is apparently vital in attaining the biological activity such reactions rapidly cascade providing complex mixtures of species. Thus, correlation of the observed cellular outcomes to a particular titanium species becomes difficult. With the aim of slowing down and controlling such hydrolysis events Tshuva has introduced polydentate phenolato ligands of type L_A and L_B.[6,7] We became intrigued as to why the related ligand cores L_C, after coordination to titanium(IV), had not been trialled in anti-cancer studies (even though examples of such complexes have been known in the fields of coordination chemistry and catalysis since 1970s).[8] We were particularly interested to see if use of ligand of type L_C could lead to highly active titanium(IV) complexes suitable for subsequent mechanistic investigations.
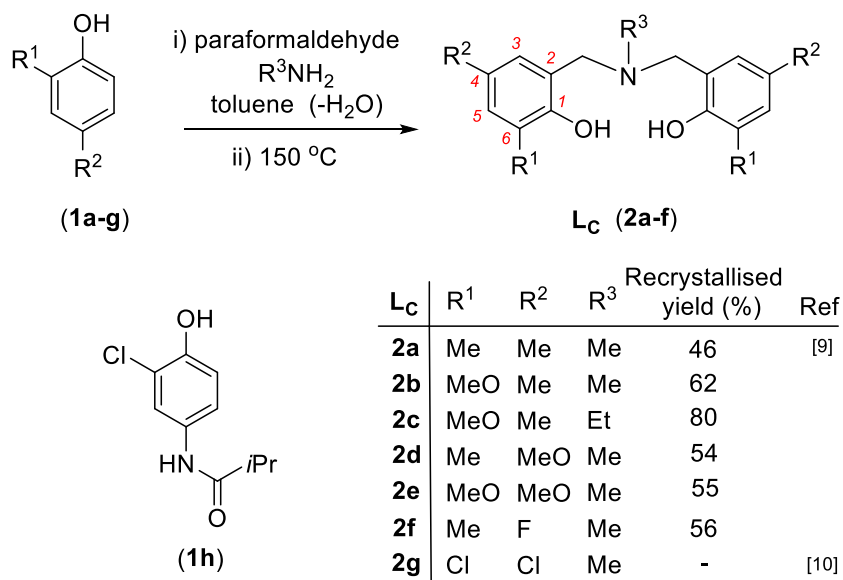

L$_A$ R = Me
L$_B$ R = CH$_2$CH$_2$OH

L$_C$ R = Me,Et
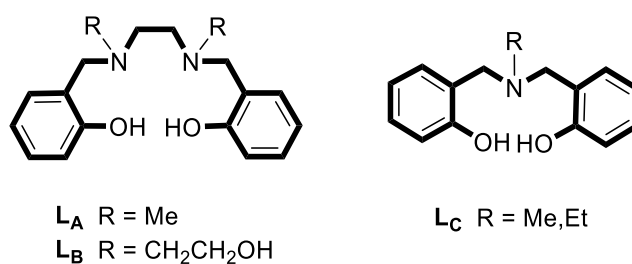
Scheme 1. Previously screened (**L$_A$**, **L$_B$**) and an untried class **L$_C$** phenolato-amine ligand cores for anti-cancer trials of titanium(IV) complexes.
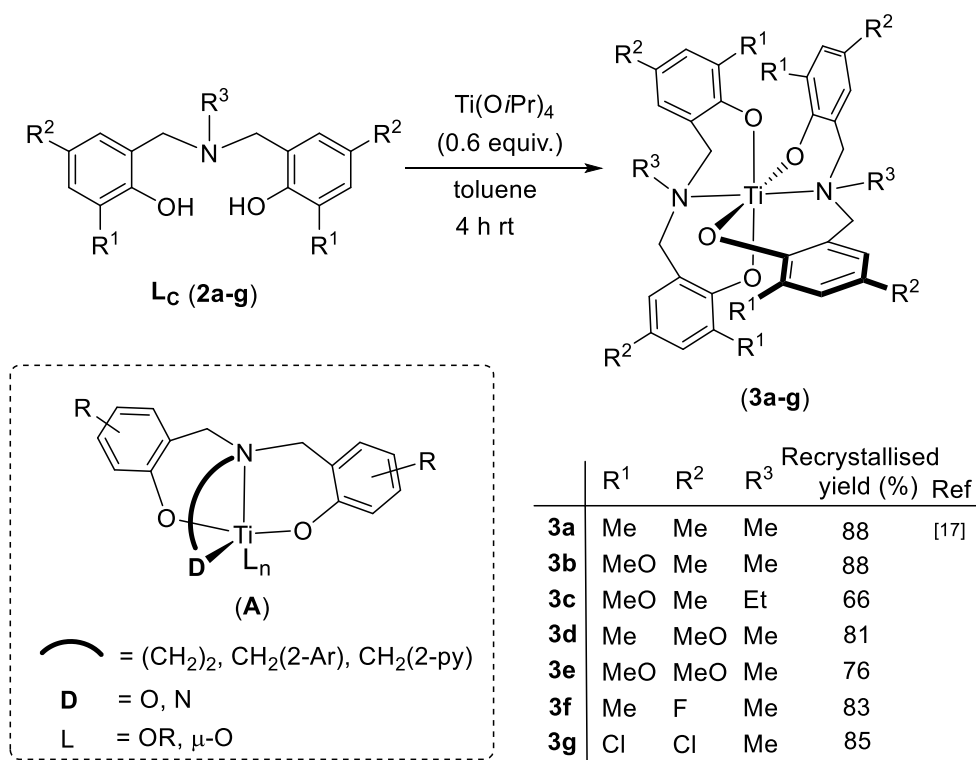
Results and Discussion

Ligand and complex formation and stability

While over 5000 examples of entities containing the sub structure core of **L$_C$** (shown in bold) are known,[8] it is desirable for biological studies (e.g. for oxidative stability) to block sites *ortho* and *para* to the phenol (OH) function and to restrict R to a simple methyl unit. Only 35 examples of such structures (**2**, Scheme 2) are known, where R^1 and R^2 are restricted to Br, Cl, Me, *t*Bu and adamantyl.[8] Importantly, *no examples* of **2** have been reported containing electron-releasing OMe units, which we postulated would be the most biologically active when R^3 = Me. We thus prepared a small library of 4,6-substituted versions of **L$_C$ 2a-f** (Scheme 2) using simple Mannich chemistry. Five moderate electron-rich ligands **2a-e** containing methyl (σ_p = -0.17) and methoxy (σ_p = -0.27) units were prepared of which only **2a** was previously known.[9] Non-commercial phenols (**1d-e**) are accessed by simple Bayer-Villiger oxidations of the parent aldehydes (see Supporting Information). Crude yields for **2a-e** were in the range 50 to 80+% and analytically pure materials were attained by layering pentane onto their ether solutions. Attempts to prepare 4,6-substituted **L$_C$** from nitrogen containing **1h** were unsuccessful (Supporting Information). For comparison electron deficient **2f** (F, σ_p = +0.06) and **2g** (Cl, σ_p = +0.23) were also targeted. While **2f** is prepared in moderate yield **2g** could not be isolated pure in our hands, although it is described in the literature.[10] However, compound **2g** is clearly present in the crude mixture and this could be used for subsequent complexation studies (see later).

L$_C$	R^1	R^2	R^3	Recrystallised yield (%)	Ref
2a	Me	Me	Me	46	[9]
2b	MeO	Me	Me	62	
2c	MeO	Me	Et	80	
2d	Me	MeO	Me	54	
2e	MeO	MeO	Me	55	
2f	Me	F	Me	56	
2g	Cl	Cl	Me	-	[10]

Scheme 2. 4,6-substituted ligand **Lc** library prepared in this study.

Reaction of ligands **2** at a 2:1 stoichiometry with Ti(O*i*Pr)$_4$ in toluene at ambient temperature leads to intense red coloured solutions from which complexes **3** can be isolated in good yield as rhomboidal crystals or orange powders upon removal of the toluene and recrystallisation from optimal solvents (see Supporting Information) (Scheme 3).

	R^1	R^2	R^3	Recrystallised yield (%)	Ref
3a	Me	Me	Me	88	[17]
3b	MeO	Me	Me	88	
3c	MeO	Me	Et	66	
3d	Me	MeO	Me	81	
3e	MeO	MeO	Me	76	
3f	Me	F	Me	83	
3g	Cl	Cl	Me	85	

Scheme 3. Titanium complexes **3** library prepared in this study and comparison to the more commonly targeted motifs (**A**).

Ligands of type **2** (**L$_C$**) complex readily to a wide variety of transition metals including: Zr,[11] V,[12] Mo,[13] Mn,[14] Fe,[15] and Cu[16] However, for titanium only the preparation of **3a** is known[17] together with three Ti(substituted-**L$_C$**)$_2$ complexes using ligands related to **2** with R^1, R^2 = Me (or its 3-isomer), tBu and R^3 = Et, nPr, CH$_2$CH$_2$NMe$_2$.[18] Other than that, the nearest related titanium complexes we could identify (ca. 180 examples[8]) were those showing the motifs (**A**) (Scheme 3), which have been prepared mostly for studies of alkene polymerisation catalysis.[8] Complexes **3** are chiral (but racemic) and this causes observation of characteristic diastereotopic aryl C-H (four ^4J coupled doublets in the range δ_H 6.61-6.44) and NCH$_2$ (at δ_H 4.85-3.30 showing ^2J ~12.8 Hz or second order behaviour) signals. Conveniently, complexes **3** are all highly crystalline so that they can be easily brought to analytical purity for both biological and mechanistic studies (see Supporting Information for individual compounds). All of the compounds **3** are stable in dmso-d$_6$ solution (10 mM) for at least 5 days at ambient conditions. Addition of excess D$_2$O, simulating the serial dilutions carried out in the biological assessments (see later), indicated that species **3** form colloidal suspensions and that hydrolysis to afford ligands **2** as the major solution species is a slow process (>1 day, see Supporting Information).

Crystallographic studies

The molecular structure of complex **3b** was determined by X-ray studies and is shown in (Figure 1). The same *trans,mer* geometry is also seen in related crystallographic studies of **3d**, **3e**, **3f** (see Supporting Information) and for the literature structure of **3a**.[17] The ligands in

4

these series **3** contain a common CH_2NMeCH_2 linker so that electronic effects on bonding to TiO_4N_2 core induced by the aryl substituents can be examined. Comparing the bond distance and angle data for these five complexes (Table 1) reveals a very similar range of geometries. No significant structural correlation of the pro-drug structures of **3** to their cytotoxic activity (see later) was observed, implying that the observed structure-activity-relationship is due only to ligand electronic effects on the electron density in *in vitro* formed titanium species. At best for precursors **3** a slight distortion of N-Ti-N angles correlated with the anti-cancer activity. However, the latter may be due to crystal packing rather than substituent effects. Complexes **3d-f** were found to crystallise as solvates, but these are readily lost in the absence of supporting solvent and all subsequent biological studies were carried out on samples of **3** assayed as solvent free (NMR) and analytically pure (CHN).
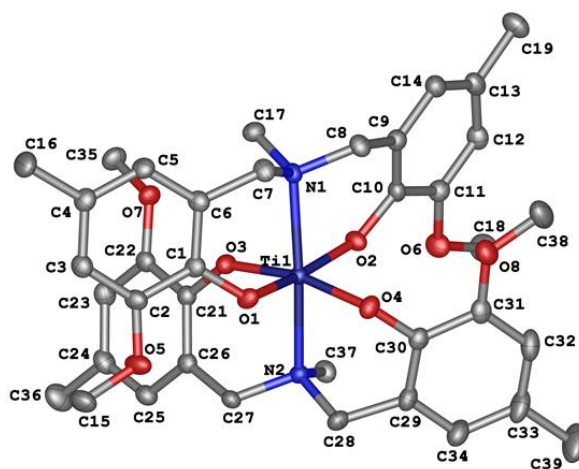

Figure 1. Molecular structure of titanium complex **3b**.

Table 1. Selected comparison of bond distance and angle data for titanium complexes **3a-3b** and **3d-f** for their TiO_4N_2 cores.[a]

Complex	3a[b]	3b[c]	3d[c]	3e	3f
R^1 (*ortho*)	Me	MeO	Me	OMe	Me
R^2 (*para*)	Me	Me	OMe	OMe	F
Bond lengths (Å)					
Ti(1)-O(1)	1.892	1.909	1.881	1.921	1.880
Ti(1)-O(2)	1.882	1.859	1.889	1.874	1.876
Ti(1)-O(3)	1.892	1.873	1.894	1.867	1.880
Ti(1)-O(4)	1.882	1.900	1.878	1.887	1.876
Ti(1)-O$_{ave}$	1.887	1.885	1.885	1.887	1.878
Ti(1)-N(1)	2.264	2.244	2.244	2.272	2.247
Ti(1)-N(2)	2.264	2.267	2.265	2.251	2.247
Ti(1)-N$_{ave}$	2.264	2.255	2.256	2.262	2.247
Bond angles (º)					
O(1)-Ti(1)-O(2)	168.6	167.5	167.1	165.2	167.9
O(3)-Ti(1)-O(4)	168.6	167.6	167.9	166.4	167.9

| N(1)-Ti(1)-N(2) | 179.7 | 174.7 | 173.8 | 173.6 | 179.8 |

[a] The TiO$_4$N$_2$ donor set is numbered in all cases as for **3b** in Figure 1 (see also Supporting Information). [b] Based on the published SEFZIN structure.[17] [c] Average of two independent molecules within unit cell.

Growth inhibitory activity of 3b-e against MCF-7 and HCT-116

In vitro antitumor activity of all compounds (**3**) was assessed using the MTT assay against two human-derived cancer cell lines: MCF-7 (breast) and HCT-116 (colon), with cisplatin as a positive control for all tests, using standard protocols (see Supporting Information). Compound **3a** has been previously reported in the literature,[17] but its anti-cancer properties were not determined. Trials of **3a** revealed unremarkable activity (GI$_{50}$ values 35-40 µM) against both these cell lines. Exchange of a single methyl for methoxy group in complex **3b** resulted in >10-fold increase in anti-cancer activity. The growth inhibitory activities of **3a** and **3b** are compared in Figure 2. The GI$_{50}$ values of the electronically diverse complexes **3b-f** were similarly screened by MTT assay. Complex **3b** was confirmed as the most active with GI$_{50}$ values of ~1 µM for MCF-7 and ~3.4 µM for HCT-116 (Table 2). Other compounds in the series showed moderate to good activity anti-cancer performance (Figure 3 and Table 2). Typically, no structural modifications were made to the compounds at the nitrogen donor (e.g. R^3), as preliminary studies changing the methyl group within **3b** to the ethyl derivative **3c** negatively affected the compound class, reducing potency. The activity of **3c** is similar to cisplatin, whose control GI$_{50}$ values in our studies were 6.6 µM for MCF-7 and 9.2 µM for HCT-116 (Figure 3A-B). We suspect **3c** of being less soluble in aqueous media leading to reduced activity. Our results show that Ti(IV) complexes **3b-f** are among the most active reported in the literature[4-7] and that this activity is strongly dependent on the ligand structure. While **3b** is the most potent compound, **3d** showed good activity with GI$_{50}$ values of 2 µM and 3 µM against MCF-7 and HCT-116 cell lines respectively (Figure 3A-B and Table 2). Complex **3e** showed lower potency than **3b** and **3d** against the same cell lines (GI$_{50}$ values ~8.5 µM against both MCF-7 and HCT-116 cells; Figure 3A-B and Table 2). Complex **3f** revealed reduced activity with GI$_{50}$ values of 11.7 µM for MCF-7 and 22 µM for HCT-116 (Figure 3A-B and Table 2).
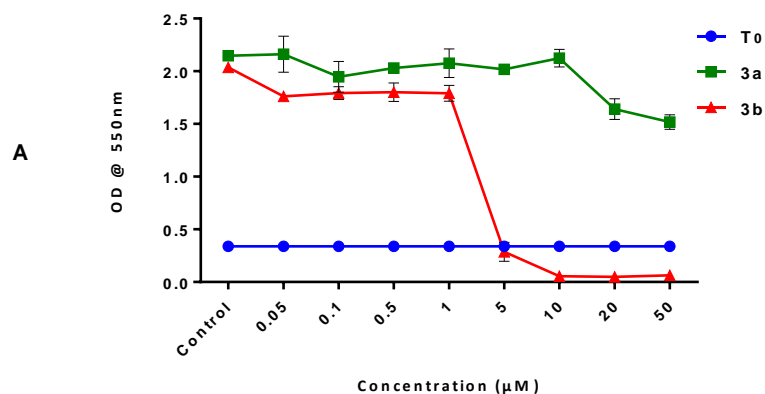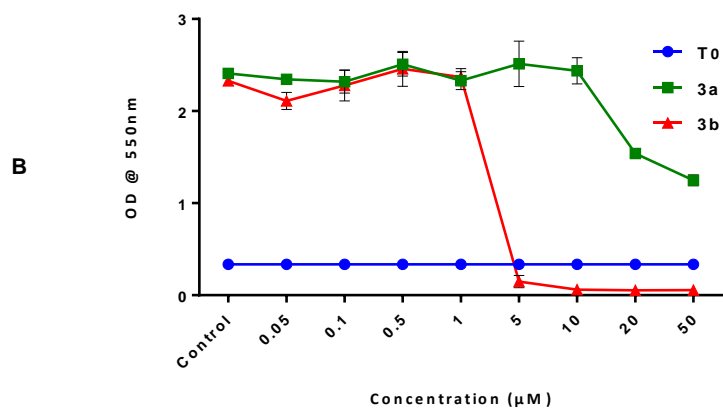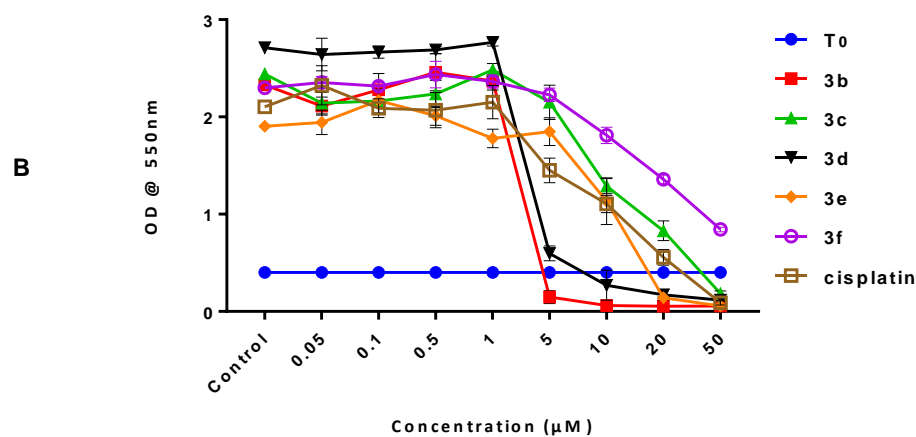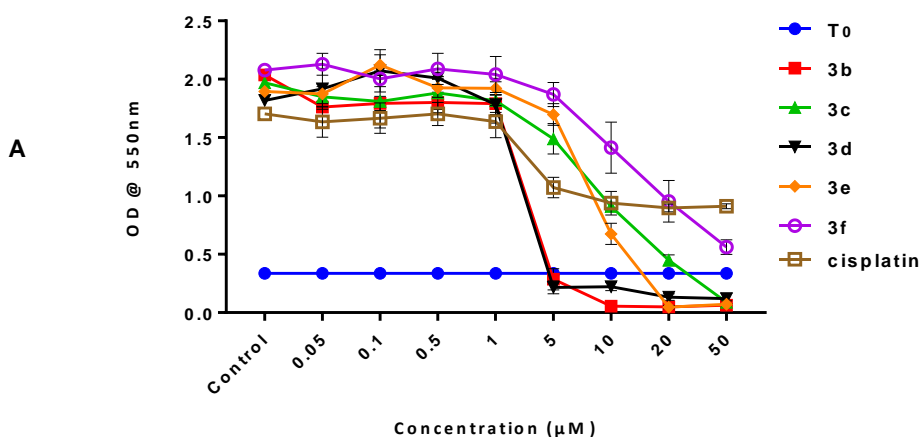
Figure 2. Representative MTT graphs displaying the dose-dependent growth inhibitory properties of **3a-b** against MCF-7 (**A**) and HCT-116 (**B**) cell lines. Cells were seeded in 96-well plates at a density of 3 x 10^3 cells/well. After allowing 24 h to adhere, cells were treated with the specified compound and incubated for 72 h. Data points depict mean ±S.D. n = 8; MTT assays were repeated >3 times. LineT_0 is a control run: using just media and cancer cell line.

Figure 3. Representative MTT graphs displaying the dose-dependent growth inhibitory properties of **3b-f** against MCF-7 (**A**) and HCT-116 (**B**) cell lines. Cells were seeded in 96-well plates at a density of 3 x 10^3 cells/well. After allowing 24 h to adhere, cells were treated with the specified compound and incubated for 72 h. Data points depict mean ±S.D. n = 8; MTT assays were repeated >3 times. LineT$_0$ is a control run: using just media and cancer cell line.

Tetrachloro analogue **3g** showed the lowest activity amongst the new derivatives of **3** screened and was comparable to complex **3a**. The **3g** GI$_{50}$ values were: 51.5 μM for MCF-7 and 64.8 μM for HCT-116 (Figure S4, see Support Information). The selectivity of **3b** to cancerous cells was evaluated by measuring its growth inhibitory activity in non-cancerous MRC-5 human lung fibroblast (Figure S5-A, see Support Information). Complex **3b** showed reduced activity (cytotoxicity) toward these cells, implying a degree of cancer cell selectivity.[19] The GI$_{50}$ value of **3b** in MRC-5 cells was higher at 7.3 μM (Table 2), indicating a ~7-fold selectivity when compared to activity against MCF-7 breast cancer cells. The activities of all Ti(IV) complexes **3** were similarly assessed against MRC-5 and consistently, reduced activities were observed against these non-tumourigenic fibroblasts; the GI$_{50}$ values for **3e**, **3f** and **3g** were ~16 μM , 34 μM and >100 μM respectively. This was in complete contrast to cisplatin controls, which were equi-active across all three cell lines (cancerous MCF-7 and HCT-116 and benign MRC-5 fibroblasts). Thus, the novel Ti(IV) complexes **3** demonstrate significant cancer cell selectivity (Table 2 and Figure S5-B in Supporting Information).

The *in vitro* growth inhibitory activity of complexes **3a-g** are summarised in Table 2. An interesting correlation is seen between the electronic properties of the phenolic substituents vs. the cellular cytotoxic activity. Moderate donation (R^1, R^2 = Me, MeO) into the phenolate results in increased activity, but if this is either further increased (**3e**) or decreased (**3a**, **3f**, **3g**) the biological activity falls. Bulky substitution of R^3 (**3b** vs. **3c**) also has a negative effect on biological performance.

Table 2. Activity of complexes **3** (GI$_{50}$ values in μM by MTT assay) against MCF-7 and HCT-116 cancer cell lines and normal MRC-5 fibroblast cells. Data were generated from ≥3 independent trials; n = 8 per experimental condition per trial.

3	R^1	R^2	R^3	σ$_p$(R^1)[a]	σ$_p$(R^2)[a]	GI$_{50}$ (MCF-7) (μM)[b]	GI$_{50}$ (HCT-116) (μM)[b]	GI$_{50}$ (MRC-5) (μM)[b]
3a	Me	Me	Me	-0.17	-0.17	36.3±0.1	38.6±0.1	>50
3b	MeO	Me	Me	-0.27	-0.17	1.0±0.04	3.4±0.07	7.33±0.04
3c	MeO	Me	Et	-0.27	-0.17	6.6±0.07	9.2±0.09	15.23±0.01
3d	Me	MeO	Me	-0.17	-0.27	2.2±0.06	3.0±0.05	8.38±0.04
3e	MeO	MeO	Me	-0.27	-0.27	8.4±0.1	8.6±0.15	16.0±0.1
3f	Me	F	Me	-0.17	+0.06	11.7±0.05	22±0.031	34±0.03
3g	Cl	Cl	Me	+0.23	+0.23	51.5±0.1	64.8±0.07	>100
Cis-Pt[c]	-	-	-	-	-	7.8±0.04	8.4±0.06	7.6±0.09

[a] Hammett parameter value for *para* substituent.[20] [b] As determined by MTT assay (3 duplicates). [c] Cisplatin.

Effect of 3b and 3d-f on MCF-7 and HCT-116 colony formation

Having established that Ti(IV) analogues **3** cause selective growth inhibitory activity in two cancer cell lines, we sought to evaluate whether these cancer cells could survive a brief challenge of 24 h exposure to 1 μM or 5 μM of representative Ti complexes **3** and retain their proliferative capacity. To this end, clonogenic assays were set up. Clonogenic assays are a recognised technique for determining the cytotoxic potential of a test agent and results are typically represented as a survival fraction (%) vs control cell colony populations of non-treated cells. Both **3b** and **3d** significantly inhibited colony formation after 24 h treatment of cells at concentrations of 1 and 5 μM (Figure 4A-B). Complexes **3b** and **3d** inhibited MCF-7 colony formation cell at 1 and 5 μM by 40-45% and 100% respectively. Despite the fact that MCF-7 and HCT-116 showed variable sensitivities to **3b** and **3d** (GI$_{50}$ 1.0 μM and 3.4 μM respectively), similar inhibition of HCT-116 colony formation was observed, 51% and 100% by 1 and 5 μM values respectively (Figure 4A-B). Complexes **3e** and **3f** also inhibited the colony formation in MCF-7 cells by 25% and 29% (1μM), and 57% and 48% (5 μM) respectively. The same agents inhibited HCT-116 colony formation by 16% and 22% (1 μM **3e** and **3f**) and 49% and 28% (5 μM **3e** and **3f**; Figure 6A-B). Complete (100%) inhibition of colony formation was observed in HCT116 cells and MCF-7 exposed to 5 μM **3b** and **3d**, reflecting potency and cytotoxicity of these complexes (Figure S6 C and D, see Support Information). These data indicate that the cancer cells have lost their ability to form progeny colonies or have been killed (Figure S6-C, see Support Information).[21] Representative colonies are shown in (Figure S6 C-D, see Support Information). In contrast, at the concentrations adopted, **3e** and **3f** demonstrated reduced potency, therefore exposure of MCF-7 or HCT-116 cells to 1 μM or 5 μM **3e** and **3f** failed to inhibit colony formation by >50%.[22]
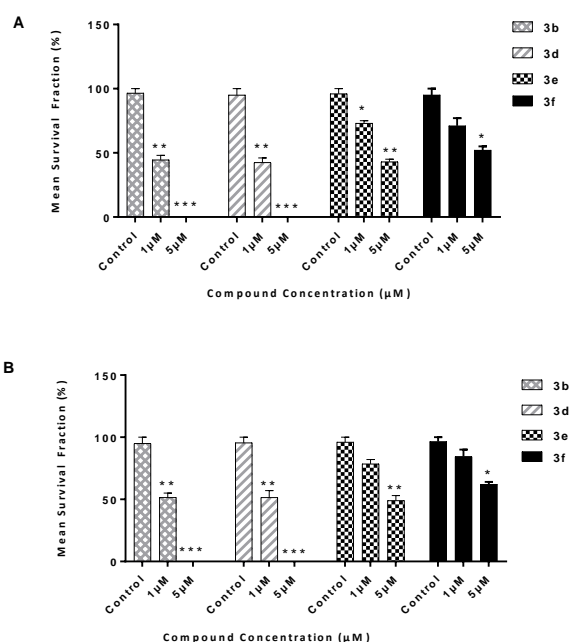

Figure 4. Effect **3b**, **3d**, **3e**, and **3f** on **A**) MCF-7, **B**) HCT-116 colony formation. A + B Mean survival fraction of % control represented of mean ±SEM of 5 independent trials (n = 2 per trial). Complexes **3b** and **3d** exhibited significant reduction in colony formation while **3e** and **3f** showed modest activity by comparison (*p* < 0.0001, n = 2).

Cell cycle analysis

Based on MTT and clonogenic assays, the complexes **3** compromise cancer cell viability and growth. Led by these observations, we examined the effect of **3b**, **3f** (as efficient and modest agents, i.e. GI_{50} values of ca. 7 and 34 μM against the HCT-116 cell line respectively), and cisplatin (as a positive control) on cell cycle perturbation by flow cytometry. An HCT-116 control cell cycle distribution profile demonstrated: 53.4 %, 24.9 % and 15.3 % events for the G1, S, G2/M phases[5] respectively. Negligible events can be detected in the preG1 compartment reflecting a healthy HCT-116 population (Figure S7, see Supporting Information). In contrast, following 72 h exposure of these cells to 10 μM (~1.5 x GI_{50}) cisplatin, a substantial pre-G1 population is evident (25.5 % events) indicative of cells undergoing apoptosis. It is known that cisplatin causes DNA inter- and intra-strand crosslinks,[23] blocking DNA replication; alerted DNA repair mechanisms fail to repair cisplatin-induced DNA damage (initially) initiating apoptosis. As DNA replication is blocked and repair is attempted, the cell cycle is halted during S and G2 phases. After 72 h of continued treatment, DNA repair failure triggers programmed cell death. No preG1 peak is evident in HCT-116 cells exposed to 10 μM (~3 x GI_{50}) **3b**; this Ti(IV) analogue caused a profound accumulation of events in the G2/M phases, indicating a different/delayed mechanism of action. If the arrested cell cycle occurs as a result of DNA damage, its onset may be later than that caused by cisplatin.[24] In contrast, complex **3f** (at 10 μM; <0.5 x GI_{50}) caused negligible apparent cell cycle perturbation. MCF-7 cells exposed to cisplatin, **3b** or **3f** demonstrated modest increase in late S/G2/M events (Supplementary Figure S8).

Induction of apoptosis in cancer cells

Annexin-V/PI apoptosis assays[5] were performed to explore the apoptosis-inducing properties of **3b** and **3f**; cisplatin being used as a positive control. MCF-7 and HCT-116 cells were exposed to both complexes (5 μM and 10 μM; 72 h). Apoptotic populations were confirmed by dual annexin V-FITC/PI staining (Figure 5). The majority (65%) of cells exposed to 10 μM cisplatin (72 h) were undergoing apoptosis. Both **3b** and **3f** revealed profound apoptotic MCF-7 and HCT-116 populations at the concentrations tested. However, while early and late apoptosis were evident in HCT-116 cells treated with **3b**, exposure to **3f** for 72 h revealed a larger proportion of cells undergoing early apoptosis – indicating later onset of programmed cell death (Figure 5, and Figures S9, S10 Supporting Information).
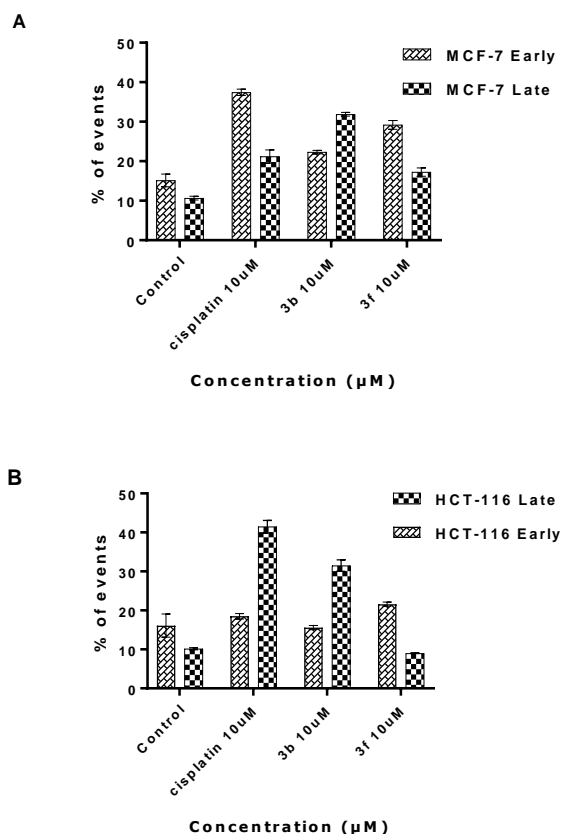
Figure 5. Apoptotic effects of **3b**, **3f** , and cisplatin on **A**) MCF-7 and **B**) HCT-116 cells at 10 µM. Cells were treated with 10 µM for 72 h. Annexin-V/PI apoptosis assay was adopted to determine the percentage of apoptotic cells.

Induction of DNA damage

To determine whether apoptosis is triggered by DNA double strand breaks (DSBs), flow cytometric analyses of control, cisplatin-, **3b-** and **3f**-treated HCT-116 and MCF-7 populations were performed following co-incubation with PI (propidium iodide) and a 1° Ab (primary antibody) recognising γ-H2AX;[5] γ-H2AX foci appear at sites of DNA DSBs.[25] It is known that cisplatin causes DNA damage: inter/intrastrand DNA crosslinks, and DNA monoadducts that lead to DNA DSBs. These harbingers of apoptosis are largely responsible for Pt-drug antitumor activity.[1,23] Thus, co-incubation of cell populations with PI and 1° Ab recognising γ-H2AX, prior to flow cytometry analyses, allows cell-cycle-specific detection of sites of DNA DSBs. Consistent with cell cycle analyses, dual PI/ γ-H2AX labelling of HCT-116 cells supported **3b**-induced G2/M cell cycle arrest. Interestingly, HCT-116 G2/M events comprised a population heavily positively stained γ-H2AX+ve (53 %) suggestive of the presence of DNA DSBs. Complex **3f**, in contrast (consistent with HCT-116 cell cycle analysis and reduced potency) revealed neither G2/M arrest, nor γ-H2AX-+ve events associated with this cell phase. Rather a minority proportion of G1 events appeared to have incurred DNA DSB damage and were γ-H2AX+ve. Validating these analyses, accumulation of G2/M cell cycle events following exposure of HCT-116 cells to cisplatin (10 µM; 72 h was observed accompanied by γ-H2AX +ve events at sites of

DNA DSBs (Figure S11, Support Information). Obvious γ-H2AX +ve events were detected in G1 and G2 cell cycle phases following exposure of MCF-7 cells to cisplatin, **3b** or **3f** (Supporting Information, Figure S12). Interestingly, chiral cyclopentadienyl complexes did not halt the cell cycle in treated cells and DNA DSBs (γ-H2AX foci) were similarly not detected.[26] Instead, antitumor activity of this compound was a consequence of paraptotic cell death, involving MAP kinase signal transduction. In contrast, current Ti complexes **3b** and **3f** clearly evoke apoptosis.

Caspase activation

Taken together, our data suggest that potent Ti-complex **3b** causes later-onset apoptosis compared to cisplatin. To irrefutably confirm an apoptotic cell fate for cells exposed to **3b**, a caspase 3/7 activation assay was performed following exposure of HCT-116 and MCF-7 cells to escalating concentrations of **3b**. Dose-dependent significant caspase activation ($\geq$5 μM **3b** p< 0.0001; Figure 6) was detected following 72 h exposure of cells to **3b** consistent with apoptosis-induction. As a positive control, 50 μM cisplatin was to confirm the assay raised caspase activation (e.g. by ~350% in HCT-116 populations; not shown). These data confirm that after 72 h exposure, **3b** triggers apoptotic cell death (Figure 6).[27]
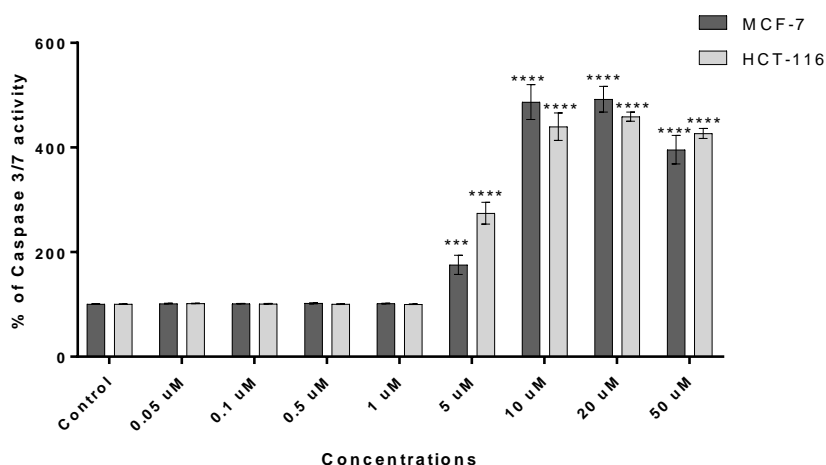

Figure 6. Dose-dependent elevation of caspase 3/7 activity in HCT-116 and MCF-7 cells following 72 h exposure of cells to Ti-complex **3b**. Data points are mean ±S.D; (p < 0.0001, n = 8).

Conclusion

A series of Ti(IV) complexes (**3**) has been synthesised and their structures confirmed by X-ray crystallography. Complex **3b** evoked potent cancer-selective growth inhibitory and cytotoxic activity. Cell cycle analyses indicated late-onset G2/M cell cycle arrest, which at 10 μM (representing ~3 x GI_{50}) triggered an apoptotic cell fate. Experiments are underway to determine modes of cell death and molecular targets of this promising class of titanium anticancer agents.

Graphical Abstract

	3b GI$_{50}$	3d GI$_{50}$
MCF-7	1.0 µM	2.2 µM
HCT-116	3.4 µM	3.0 µM
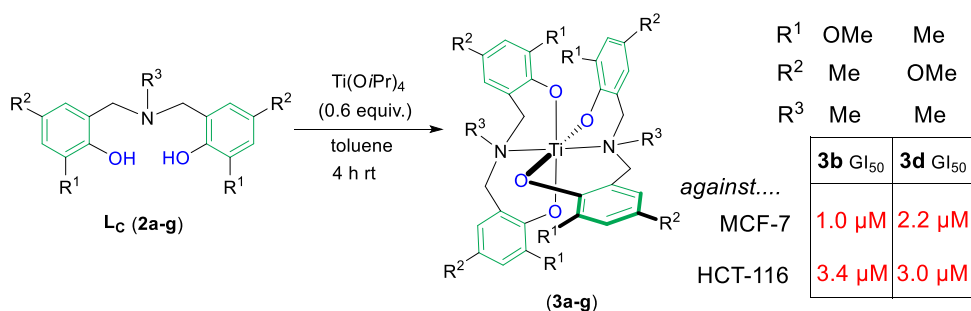
Keywords: • Antiproliferation • Cytotoxicity • Titanium • Phenolato • MCF-7 • HCT-116 • Cell cycle • Annexin V • γ-H2AX • Caspase • DNA DSBs

References

[1] For leading overviews of Pt-agents see: (a) E. R. Jamieson, S. J. Lippard, *Chem. Rev.* **1999**, *99*, 2467–2498. (b) J. S. Saad, M. Benedetti, G. Natile, L. G. Marzilli, *Inorg. Chem.* **2010**, *49*, 5573-5583 and citations thereof.

[2] For introductions to metal (including non-Pt) anti-cancer agents see: (a) *Metal-based Anticancer Agents*, Eds. A. Casini, A. Vessières, S. M. Meier-Menches, Royal Society of Chemistry, Cambridge, UK, 2019, pp 500. (b) U. Ndagi, N. Mhlongo, M. E. Soliman, *Drug Des. Devel. Ther.* **2017**, *11*,599-616. (c) M. J. Clarke, F. Zhu, D. R. Frasca, *Chem. Rev.* **1999**, *99*, 2511-2534.

[3] D. R. Williams, *Chem. Rev.* **1972**, *72*, 203-213.

[4] For overviews of titanium anti-cancer agents see: (a) E. Y. Tshuva, J. A. Ashenhurst, *Eur. J. Inorg. Chem*. **2009**, 2203-2218. (b) K. Strohfeldt, M. Tacke, *Chem. Soc. Rev.* **2008**, *37*, 1174-1187. (c) K. M. Buettner, A. M. Valentine, *Chem. Rev.* **2012**, *112*, 1863-1881. (d) S. A. Loza-Rosas, M. Saxena, Y. Delgado, K. Gaur, M. Pandrala, A. D. Tinoco, *Metallomics* **2017**, *9*, 346-356.

[5] M. Cini, T. D. Bradshaw, S. Woodward, *Chem. Soc. Rev.* **2017**, *46*, 1040-1051.

[6] (a) M. Shavit, D. Peri, C. M. Manna, J. S. Alexander, E. Y. Tshuva, *J. Am. Chem. Soc.* **2007**, *129*, 12098-12099. (b) D. Peri, S. Meker, M. Shavit, E. Y. Tshuva, *Chem. Eur. J.* **2009**, *15*, 2403-2415. (c) S. Meker, O. Braitbard, M. D. Hall, J. Hochman, E. Y. Tshuva, *Chem. Eur. J.* **2016**, *22*, 9986-9995.

[7] For recent relevant developments in the titanium anti-cancer agent area see: (a) R. Manne, M. Miller, A. Duth, M. F. C. G. da Silva, E. Y. Tshuva, T. S. B. Baul, *Dalton Trans.* **2019**, *48*, 304-314. (b) N. Ganot, O. Briaitbard, A. Gammal, J. Tam, J. Hochman, E. Y. Tshuva, *ChemMedChem* **2018**, *13*, 2290-2296. (c) M. Miller, E. Y. Tshuva, *Nature Sci. Rep.* **2018**, *8*, 9705. (d) S. A. Loza-Rosas, A. M. Vazquez-Salgado, K. I. Rivero, L. J. Negron, Y.

Delgado, J. A. Benjamin-Rivera, A. L. Vazquez-Maldonado, T. B. Parks, C. Munet-Colon, A. D. Tinoco, *Inorg. Chem.* **2017**, *56*, 7788-7802. (e) S. Barroso, A. M. Coelho, S. Gómez-Ruiz, M. J. Calhorda, Z. Zizak, G. N. Kaluđerović, A. M. Martins, *Dalton Trans.* **2014**, *43*, 17422-17433.

[8]   Substructures **L$_C$** were identified through Scifinder (May 2019). Prepared by simple Mannich chemistry, use in attaining catalysts for the polymerisation of alkenes and lactones is common; representative examples: (a) A. Lehtonen, R. Sillanpaeae, *Inorg. Chem.* **2004**, *43*, 6501-6506. (b) C.-T. Chen, C.-A. Huang, B.-H. Huang, *Macromolecules* **2004**, *37*, 7968-7973. (c) C. M. Silvernail, L. J. Yao, L. M. R. Hill, M. A. Hillmyer, W. B. Tolman, William B. *Inorg. Chem.* **2007**, *46*, 6565-6574. (d) A. Lehtonen, H. Balcar, J. Sedlacek, R. Sillanpaeae, *J. Organomet. Chem.* **2008**, *693*, 1171-1176.

[9]   W. J. Burke, J. L. Bishop, E. L. Mortensen Glennie, W. N. Bauer, *J. Org. Chem.* **1965**, *30*, 3423-3427.

[10]   W. J. Burke, E. L. M. Glennie, C. Weatherbee, *J. Org. Chem.* **1964**, *29*, 909-912.

[11]   For example: A. J. Chmura, M. G. Davidson, M. D. Jones, M. D. Lunn, M. F. Mahonc, *Dalton Trans.* **2006**, 887-889.

[12]   For example: D. Maity, J. Marek, M.-F. Sheldrick; M. Ali, *J. Mol. Catal. A* **2007**, *270*, 153-159.

[13]   For example: A. Peuronen, A. Lehtonen, *Topics Catal.* **2016**, *59*, 1132-1137.

[14]   For example: T. Weyhermüller, T. K. Paine, E. Bothe, E. Eberhard; E. Bill, P. Chaudhuri, *Inorg. Chimica Acta* **2002**, *337*, 344-356.

[15]   For example: T. Weyhermüller, R. Wagner, P. Chaudhuri, *Eur. J. Inorg. Chem.* **2011**, 2547-2557.

[16]   S. Phongtamrug, K. Tashiro, M. Miyata, S. Chirachanchai, *J. Phys. Chem.* B, **2006**, *110*, 21365-21370.

[17]   (a) A. J. Chmura, M. G. Davidson, M. D. Jones, M. D. Lunn, M. F. Mahon, *Dalton Trans* **2006**, 887-889. (b) Y. Chung, Y. Kim, *Acta Cryst. Sec. E:* **2013**, *69*, m222. (c) The Cambridge Crystallographic Data Centre (www.ccdc.cam.ac.uk) codes for these published structures of **3a** are SEFZIN and WHIMAD respectively.

[18]   D. Peri, S. Meker, C. M. Manna, E. Y. Tshuva, *Inorg. Chem.* **2011**, *50*, 1030-1038. This includes the CCDC structures REZRET: Ti{**L$_C$(2)**}$_2$ R^1 = R^2 = Me; R^3 = Et; REZRIX: Ti{**L$_C$(2)** **L$_C$(2')**} first ligand with R^1 = R^2 = Me; R^3 = Et and second ligand with R^1 = R^2 = *t*Bu; R^3 = Et and REZRUJ: Ti{**L$_C$(2)** **L$_C$(2')**} first ligand with R^1 = Me (but in 3-position) R^2 = Me; R^3 = CH$_2$CH$_2$NMe$_2$ and second ligand with R^1 = R^2 = *t*Bu; R^3 = Et.

[19]   For a related selectivity study see ref. 6c.

[20]   C. Hansch, A. Leo, R. W. Taft, *Chem. Rev.* **1991**, *91*, 165-195.

[21]   For a related example see: M. E. Qazzaz, V. J. Raja, K.-H. Lim, T.-S. Kam, J. B. Lee, P. Gershkovich, T. D. Bradshaw, *Cancer Lett.* **2016**, *370*, 185-197.

[22]   For a related example see: V. J. Raja, K.-H. Lim, C.-O. Leong, T.-S. Kam, T. D. Bradshaw, *Invest New Drugs* **2014**, *32*, 838-850.

[23]   For an overview of DNA-drug interactions see: D. Yang, J. Reedijk, G. A. van der Marel, A. H. J. Wang, *J. Biomol. Struct. Dyn.* **1996**, *13*, 989-998.

[24]   For a recent related G2 block observation see: T. Pesch, H. Schuhwerk, P. Wyrsch, T. Immel, W. Dirks, A. Bürkle, T. Huhn, S. Beneke, *BMC Cancer* **2016**, *16*, 469.

[25]   L. J. Kuo, L.-X. Yang, *In Vivo* **2008**, *22*, 305-309.

[26]   (a) M. Cini, T. D. Bradshaw, S. Woodward, W. Lewis, *Angew. Chem. Int. Ed*. **2015**, *54*, 14179-14182. (b) M. Cini, H. Williams, M. W. Fay, M. S. Searle, S. Woodward, T. D. Bradshaw, *Metallomics* **2016**, *8*, 286-297.

[27]   R. U. Jänicke, *Breast Cancer Res. Treat.* **2009**, *117*, 219-221.